Heliyon 9 (2023) e19772

Contents lists available at ScienceDirect

Heliyon

journal homepage: www.cell.com/heliyon

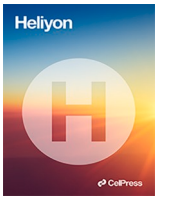

Inhibitory activity of lignanamides isolated from hemp seed hulls (*Cannabis sativa* L.) against soluble epoxide hydrolase

Jang Hoon Kim *, Yun-Chan Huh, Mok Hur, Woo Tae Park, Youn-Ho Moon, Tae IL. Kim, Seon Mi Kim, Sung-Cheol Koo

Department of Herbal Crop Research, National Institute of Horticultural & Herbal Science, RDA, Eumsung, Chungbuk, 27709, Korea

ARTICLE INFO

Keywords:
Hemp seed hulls
Lignanamide
Soluble epoxide hydrolase
Competitive inhibitor

ABSTRACT

Soluble epoxide hydrolase (sEH) is a therapeutic target for inflammation. In the present study, we isolated one new (**1**) and four known (**2**–**5**) compounds from the ethyl acetate fraction of hemp seed hulls. Their structures were elucidated as lignanamides via nuclear magnetic resonance and mass spectral analyses. All five compounds inhibited sEH activity, with half-maximal inhibitory concentrations of 2.7 ± 0.3 to 18.3 ± 1.0 μM. These lignanamides showed a competitive mechanism of inhibition via binding to sEH, with k_i values below 10 μmol. Molecular simulations revealed that compounds **1**–**5** fit stably into the active site of sEH, and the key amino acid residues participating in their bonds were identified. It was confirmed that the potential inhibitors **4** and **5** continuously maintained a distance of 3.5 Å from one (Tyr383) and four amino (Asp335, Tyr383, Asn472, tyr516) residues, respectively. These findings provide a framework for the development of naturally derived sEH inhibitors.

1. Introduction

Hemp (*Cannabis sativa* L.; family Cannabaceae) is an annual herbaceous plant originating from Central Asia that has been cultivated for approximately 4000 years as a source of food, fiber, and medicine [1–3]. Hemp seed is composed of 25–34% oil, 25–30% protein, and 30–40% fiber, and contains vitamins, minerals, and other compounds [1,4]. Hemp seed oil comprises polyunsaturated linoleic and α-linolenic acids in a 3:1 ratio, and has been reported to have anti-atherosclerotic effects by controlling serum lipid profiles and inflammatory responses, and increasing endothelial cell integrity and arterial lipid deposition [5]. Lignanamides (primarily caffeoyltyramine, cannabisin A, and cannabisin B) have been identified in the ethyl acetate fraction of defatted hemp seeds [6], which exhibit antioxidant and anti-acetylcholinesterase activities [7].

Soluble epoxide hydrolase (sEH; EC: 3.2.2.10) belongs to the α/β-hydrolase family of enzymes and is a bifunctional 120-kDa homodimeric enzyme with C-terminal epoxide hydrolase and N-terminal phosphatase activities [8]. The 35-kDa C-terminal hydrolase has been shown to hydrolyze epoxyeicosatrienoic acids (EETs) into dihydroxyeicosatrienoic acids [9]. Four regioisomeric EETs (5, 6-EET, 8,9-EET, 11,12-EET, and 14,15-EET), which are endothelium-derived hyperpolarizing factors, have anti-inflammatory activity [10]. Moreover, sEH inhibitors have shown anti-hypertensive, anti-diabetic, and anti-inflammatory activities [11]. For instance, the sEH inhibitor 12-(3-adamantane-1-yl-ureido)-dodecanoic acid (AUDA) showed inhibitory effects at nanomolar concentrations [12]. However, its use is restricted due to side effects, which include metabolic instability and limited water solubility [12]. Recently,

* Corresponding author.
E-mail addresses: jhkim53@korea.kr, oasis5325@gmail.com (J.H. Kim).

https://doi.org/10.1016/j.heliyon.2023.e19772
Received 28 May 2023; Received in revised form 29 August 2023; Accepted 31 August 2023
Available online 14 September 2023

coronavirus disease was suggested to be associated with sEH expression in various tissues [13]. In animal models, sEH inhibitors maintained EET levels and relieved lung inflammation [14].

The aim of this study was to develop naturally derived sEH inhibitors from *C. sativa*. To this end, we isolated one new (**1**) and four known (**2**–**5**) compounds via column chromatography from the ethyl acetate fraction of hemp seed hulls. Their chemical structures were identified as lignanamides via nuclear magnetic resonance (NMR) and mass spectral analyses. Further analyses confirmed competitive binding of all five compounds with sEH. The present work supports lignanamides as promising candidates for the development of novel sEH inhibitors.

2. Materials and methods

2.1. General experimental procedures

The solvents used for separation (methanol, *n*-hexane, chloroform, and ethyl acetate) were purchased from Duksan General Science (Seoul, Republic of Korea). Chromatographic separations were performed via thin layer chromatography (TLC) using glass plates pre-coated with silica gel 60 F_{254} and silica gel RP-18 F_{254} (20 × 20 cm; Merck, Darmstadt, Germany), which were visualized under ultraviolet light at 254 nm and 365 nm, respectively. For TLC, 10% ethanol–sulfuric acid was used as the color reagent. Column chromatography was carried out using 230–400-mesh silica gel 60 (Merck, Darmstadt, Germany) and 12-nm ODS-A (YMC, Kyoto, Japan) columns. NMR experiments were carried out using Bruker Avance III 400 MHz and Avance 500 MHz spectrometers (Bruker, Billerica, MA, USA). The mass spectral data were obtained using an LCMS-2020-EV with electrospray ionization (Shimadzu, Kyoto, Japan). Tris (B9754) and bovine serum albumin (BSA) (A8806) were achieved at Sigma-Aldrich (St. Louis, MO, USA). sEH (10011669), 3-phenyl-cyano(6-methoxy-2-naphthalenyl)methyl ester-2-oxiraneacetic acid (PHOME, 10009134), and positive control (AUDA, 10007972) were purchased from Cayman Chemical (Ann Arbor, MI, USA).

2.2. Plant material

Hemp seed hulls were obtained from Jay Hemp Korea (Andong-Si, Gyeongsangbuk-do, Korea) and taxonomically identified by Ph. J.H. Kim. A voucher specimen (CSSH 220726_1) was deposited at the herbarium of the Department of Herbal Crop Research, National Institute of Horticultural and Herbal Science, Korea.

2.3. Extract preparation and fractionation

Hemp seed hulls (1000 g) were extracted twice with ethanol (50 L) for a total of 10 days. The methanol fraction was extracted via vacuum evaporation (yield: 970 g). The residue was suspended in 3 L of water and partitioned sequentially into *n*-hexane (50 L, 720 g), chloroform (50 L, 110 g), ethyl acetate (50 L, 59 g), and water (78 g) fractions. The ethyl acetate fraction was subjected to normal phase column chromatography with a gradient solvent system of *n*-hexane and ethyl acetate (100:0 to 40:1), which yielded ten fractions (E1–E8). Fraction E4 was separated on a C-18 column using a gradient solvent system of water and methanol (20:0 to 1:1.5), which yielded compounds **1** (12 mg) and **2** (20 mg), and four fractions (E41–E44). Compounds **3** (150 mg) and **4** (25 mg) were isolated via C-18 column chromatography with a gradient solvent system of water and methanol (2:1 to 1:2) from fraction E42. Fraction E5 was subjected to C-18 column chromatography using an isocratic solvent system of water and methanol (21:1 to 1:4), yielding three fractions (E51–E53). Fraction E52 was separated on a silica gel column using a gradient system of chloroform and methanol (20:1 to 7:3), yielding compound **5** (31 mg).

2.4. sEH activity assay

Enzymatic assays were performed according to a previously described method [15], with modifications. The inhibition rates of the inhibitors toward sEH were determined via fluorescence measurements of the sEH with substrate PHOME. In 96-well plates, 0.13 mL of recombinant human sEH (250 ng/mL) in buffer [25 mM Tris–HCl (pH 7.0) containing 0.1 mg/mL BSA] was mixed with 0.02 mL of sample in methanol, and then 0.05 mL of 20 μM substrate was added. The amount of product converted from the substrate by the enzyme was measured using a fluorescence photometer (excitation filter: 330 nm, emission filter: 465 nm). The percentage inhibition was calculated as follows:

$$\text{inhibitory rate } (\%) = 100 - [(S_{60} - S_0) \ / \ (C_{60} - C_0)] \times 100$$

where C_{60} and S_{60} are the fluorescence of the blank (C) and isolated compounds (S) after 60 min, and S_0 and C_0 are the fluorescence of the control and inhibitor at 0 min, respectively.

2.5. Molecular docking prediction of the inhibitor–sEH binding sites

3D structures of the inhibitors were constructed and minimized using Chem3D Pro (CambridgeSoft, Cambridge, MA, USA). sEH pdb file (ID: 3ANS) was downloaded from the RCSB Protein Data Bank. Water and 4-cyano-N-[(1S,2R)-2-phenylcyclopropyl]benzamide were excluded from pdb file. Hydrogen and gasteiger charge were added to the protein using AutoDockTools (Scripps Research, La

Jolla, CA, USA). Flexible ligand docking specified torsion trees by detecting torsional roots and rotatable bonds.

The docking position was set to a size (60 × 60 × 60 at 0.375 Å) into the active site. The results were calculated via a Lamarckian genetic algorithm with the maximum number of evaluations. They were visualized using Chimera ver. 1.14 (University of California, San Francisco, San Francisco, CA, USA), and LigPlot (European Bioinformatics Institute, Hinxton, UK) [15].

2.6. Molecular dynamics of predicted docking

Molecular dynamics analysis was performed as described previously [15]. The Gromacs software was used to calculate the complex of enzyme with lignanamides. The enzyme was charged by a CHARMM all-atom force field. str. File of lignanamide by GGenFF server was converted to gro. and itp. files with CHARMM36-ff. The charged sEH-lignanamide complex was dissolved in a cubic box with H_2O and sodium using the simple point charge. The complex was minimized to a maximal force of 10 kJ/mol using the steepest-descent method, and then further equilibrated by 300 K NVT in 1 bar NPT for 100 ps. Finally, a molecular dynamics simulation was calculated for 30 ns. The results were analyzed using g_utility. The data were visualized using SigmaPlot (San Jose, CA, USA) and Chimera (San Francisco, CA, USA).

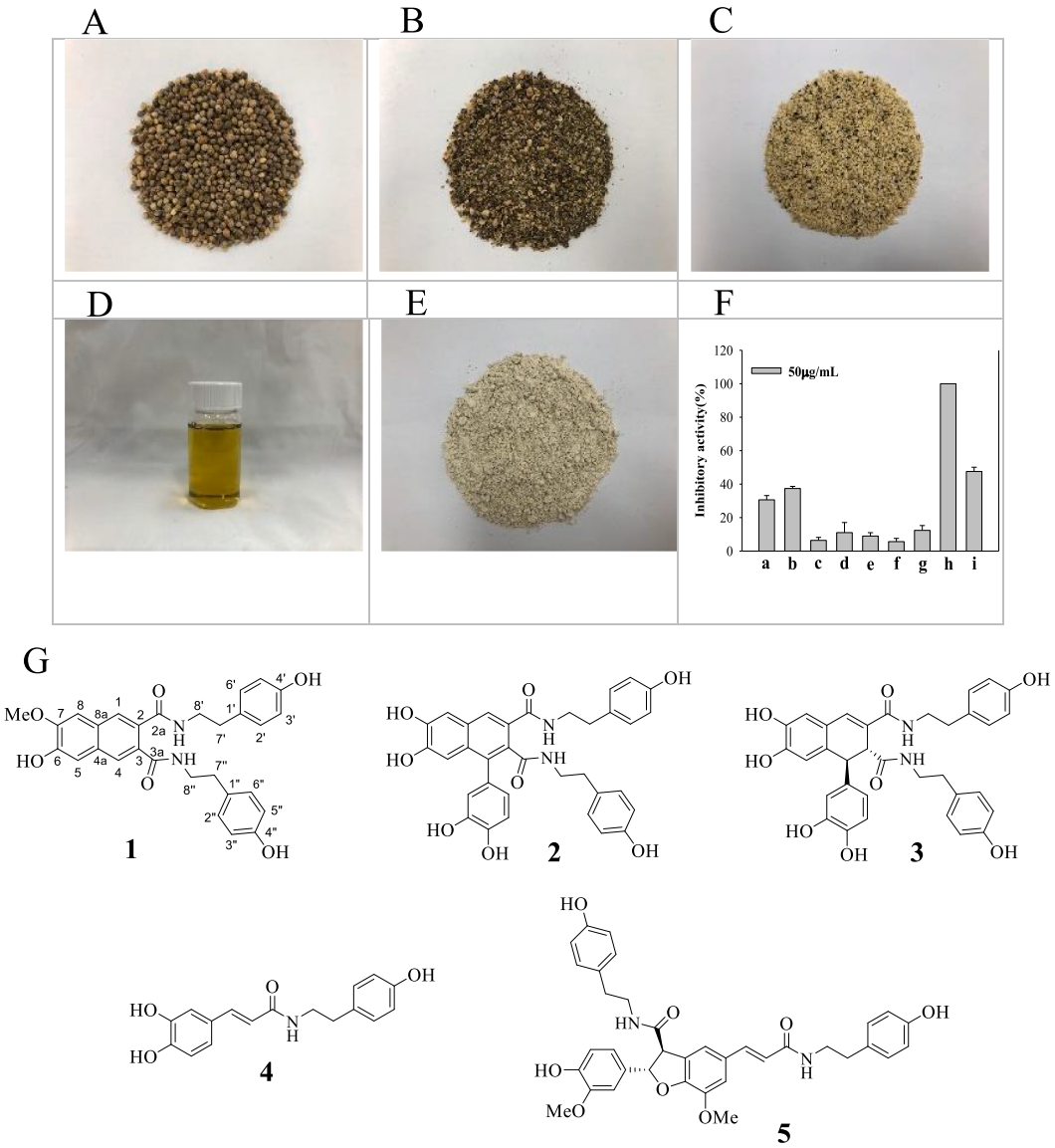

Fig. 1. Food materials derived from hemp seeds. Inhibitory activity of them (A: Hemp seeds, B: Hulls, C: dehulled seeds, D: Oil, E: cake(defatted dehulled seeds) and divided fractions (f: hexane, g: chloroform, h: ethyl acetate, i: water fraction) toward sEH (F). The structures of compounds **1**–**5** derived from the ethyl acetate fraction of the hulls extract (G).

2.7. Statistical analysis

All measurements were performed in triplicate across three independent experiments, and the results are shown as mean ± standard error of the mean (SEM). The results were analyzed using Sigma Plot (Systat Software Inc., San Jose, CS, USA).

3. Results

3.1. Compounds 1–5 derived from hemp seed hulls

Hemp seeds, hull, nut, seed oil, and cake, as food ingredients derived from hemp seed, were extracted with ethanol; the resulting extracts at concentrations of 50 μg/mL showed sEH inhibitory activities of 30.6 ± 2.5%, 37. ±1.2%, 6.3 ± 1.8%, 11.0 ± 6.0%, and 8.9 ± 2.0%, respectively (Fig. 1A–F, Table 1). Subsequently, the hemp seed hull ethanol extract was sequentially divided into *n*-hexane, chloroform, ethyl acetate, and water fractions. The ethyl acetate fraction exhibited greater inhibitory activity (>100%) than the other fractions (*n*-hexane: 5.6 ± 1.9%; chloroform: 12.3 ± 2.8%; ethyl acetate: >100%, water: 47.5 ± 2.5%) (Fig. 1F, Table 2).

Based on its relatively high bioactivity, the ethyl acetate faction was further separated via silica gel and C-18 column chromatography into one new (**1**) and four known (**2**–**5**) compounds. Their structures were elucidated via 1D- or 2D-NMR analysis as follows: cannabisin I (**1**), cannabisin A (**2**) [16], cannabisin B (**3**) [17], *N-trans*-caffeoyltyramine (**4**) [16,17], and grossamide (**5**) [16] (Fig. 1G).

Compound **1** was a white power. The molecular formula was determined to be $C_{29}H_{28}N_2O_6$ based on a pseudo-molecular ion peak $[M+H]^+$ at 501.2019 *m/z* (calculated as 501.2020) via high-resolution electrospray ionization mass spectrometry. The ^{1}H NMR spectrum indicated the presence of twelve aromatic [δ_H 7.70 (1H, s), 7.63 (1H, s), 7.25 (1H, s), 7.16 (1H, s), 7.13 (2H, d, J = 8.5 Hz), 7.12 (2H, d, J = 8.5 Hz), 6.76 (2H, d, J = 8.5 Hz), 6.76 (2H, d, J = 8.5 Hz)], one methoxy [δ_H 4.00 (3H, s)], and eight methylene [δ_H 3.54 (4H, m), 2.85 (4H, m)] signals. The ^{13}C NMR and DEPT-135 spectra revealed carbon signals, including two ketone (δ_C 172.3, 172.2), twenty-two aromatic (δ_C 157.1, 152.0, 150.3, 148.7, 132.5, 131.9, 131.5 × 2, 131.0 × 4, 131.0, 130.1, 127.9, 127.2, 116.4 × 4, 111.2, and 107.7), one methoxy (δ_C 56.5), and two methylene (δ_C 43.0, 35.7) carbons. The COSY spectrum showed correlations of the H-2′/H-6′ aromatic signal (δ_H 7.13) with the H-3′/H-5′ aromatic signal (δ_H 6.76), the H-2′′/H-6″ aromatic signal (δ_H 7.12) with the H-3′′/H-5″ aromatic signal (δ_H 6.74), and the H-8′/H-8″ methylene signal (δ_H 3.54) with the H-7′/H-7″ methylene signal (δ_H 2.85) (Fig. 2). The HMQC spectrum revealed four singlet [δ_H 7.70 (1H), 7.63 (1H), 7.25 (1H), 7.16 (1H)], four doublet [δ_H 7.13 (2H), 7.12 (2H), 6.76 (2H), 6.74 (2H)], one singlet [δ_H 4.00 (3H)], and two multiple [δ_H 3.54 (4H), 2.85 (4H)] proton signals correlated with 11 carbon signals. In the HMBC spectrum, the H-1 and H-4 signals were correlated with the C-2a ketone and C-8, and C-3a ketone and C-5 signals, respectively; the H-8 and H-5 aromatic signals were correlated with the C-7 signal corresponding to the methoxy signal (δ_H 4.00); H-8′ and H-8″ had a co-relationship with the C-2a ketone and C-7′ methylene signals, and C-3a ketone and C-7″ methylene signals, respectively; and the H-7′ and H-7″ methylene signals were correlated with the C-2′/3′ and C-2′′/3″ signals, respectively (Fig. 2, Table 2). Additionally, the carbon assignments were compared with the carbon signal assignments of compound **2**. Finally, the structure of compound **1** was elucidated as 6-hydroxy-7-methoxy-N2, N3-bis[2-(4-hydroxylphenyl)ethyl] naphthalene-2,3-dicarboxamide, and named cannabisin I.

3.2. Inhibitory activities of compounds 1–5 against sEH

Five compounds (**1**–**5**) derived from hemp seed hulls were evaluated for their degree of inhibition of sEH activity. AUDA was used as a positive control, which had a half-maximal inhibitory concentration (IC_{50}) of 24.1 ± 0.1 nM. To calculate their IC_{50} values,

Table 1
The inhibitory activity of extracts and fraction and molecular docking compounds 1–5 on sEH.

	Inhibitory activity at 50 μg/mL(%)[a]	I	IC_{50} value (μM)[a]	Inhibition type(K_i, μM)	Autodockscore(kcal/mol); Hydrogen bonds(Å)
a	30.6 ± 2.5	**1**	8.9 ± 0.8	Competitive (9.0 ± 0.8)	−10.96; Asp335(2.71), Ile363(3.03), Gln384(3.09)
b	37.4 ± 1.2				
c	6.3 ± 1.8	**2**	18.3 ± 1.0	Competitive (6.9 ± 0.7)	−11.20; Asp335(2.96), Tyr343(2.72), Ile363(2.83, 2.88), Pro371(2.76, 3.00)
d	11.0 ± 6.0				
e	8.9 ± 2.0				
f	5.6 ± 1.9	**3**	8.3 ± 1.1	Competitive (9.9 ± 0.8)	−10.69; Tyr343(2.71), Ile363(3.01), Pro371(2.71, 2.86)
g	12.3 ± 2.8	**4**	3.2 ± 0.4	Competitive (1.8 ± 0.4)	−8.48; Asp335(2.83), Leu408(2.87, 3.11)
h	>100	**5**	3.3 ± 0.3	Competitive (1.5 ± 0.2)	−14.80; Asp335(2.59), Tyr383(2.81), Gln384(2.93), Ile363(2.98), Trp473 (2.85), Met469(2.57)
i	47.5 ± 2.5	**6**[b]	24.1 ± 0.1 nM		

a: seed, b: hull, c: nut, d: Oil, e: cake, f: *n*-hexane fraction, g: Chloroform, h: ethyl acetate, i: water.
[a] All compounds examined in a set of triplicated experiment.
[b] Positive control(AUDA).

Table 2
^{1}H and ^{13}C NMR data of compound **1** in CD_3OD (500 MHz and 125 MHz).

Compound 1		
.	δ_C	δ_H
1	172.2	7.70(s)
2	131.0	
2a	172.3	
3	131.0	
3a	172.2	
4	127.9	7.63(s)
4a	131.9	
5	111.2	7.16(s)
6	148.7	
7	150.3	
8	107.7	7.25(s)
8a	132.5	
1′	131.5	131.5
2′,6′	131.0	7.13(d, J = 8.5Hz)
3′,5′	116.4	6.76(d, J = 8.5Hz)
4′	157.1	
7′ 7″	35.7	2.93–2.80(m)
8′ 8″	43.0	3.54(m)
1″	131.5	131.5
2″,6″	131.0	7.12(d, J = 8.5Hz)
3″,5″	116.4	6.74(d, J = 8.5Hz)
4″	152.0	
7-OMe	56.5	4.00(s)

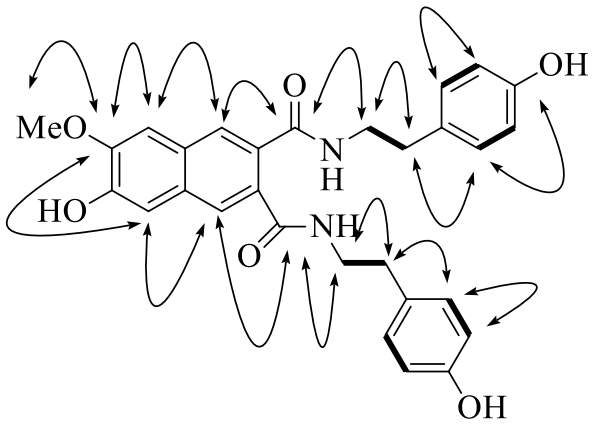

Fig. 2. Key HMBC(→) and COSY(—)correlations of compound **1**.

compounds **1**–**5** were evaluated for sEH inhibitory activity at concentrations of 1.56–50 μM. Compounds **1**–**5** showed inhibitory activity in a dose-dependent manner, with IC_{50} values ranging from 3.2 ± 0.3 to 18.3 ± 1.0 μM (Fig. 3A, Table 1).

Enzyme kinetics analysis was performed to confirm the binding mode between sEH and the lignanamides. We established several concentrations at which the compounds had inhibitory activity against sEH. At a single concentration, a linear equation was derived from the difference in the initial velocity (v_o) according to various concentrations of substrate. The resulting linear equations for the inhibitors passed through a point at $1/V_{max}$ and had different negative $1/K_m$ values. This pattern in Lineweaver–Burk plots is typical of a competitive reaction of an inhibitor against an enzyme (Fig. 3B–F, Table 1). The calculated inhibition constants (k_i) of compounds **1**–**5** ranged from 1.5 ± 0.2 to 9.9 ± 0.8 μM (Fig. 3G–K).

3.3. Molecular docking prediction of the inhibitor–sEH binding sites

In drug discovery, it is important to understand the formation mechanism of enzyme–inhibitor complexes. Therefore, we performed molecular docking experiments to predict the binding behaviors of the competitive inhibitors with sEH. Compounds **1**–**5** fit stably into the active site of sEH, with AutoDock scores of −10.96, −11.2, −10.69, −8.48, and −14.80 kcal/mol, respectively (Fig. 4A, Table 1). Additionally, hydrogen bonding, which generally has an important role in the binding of inhibitors to sEH, was identified. Compounds **1**–**5** had three (Asp335 at 2.71 Å, Ile363 at 3.03 Å, and Gln384 at 3.09 Å), four (Asp335 at 2.96 Å, Tyr343 at 2.72 Å, Ile363 at 2.83 Å

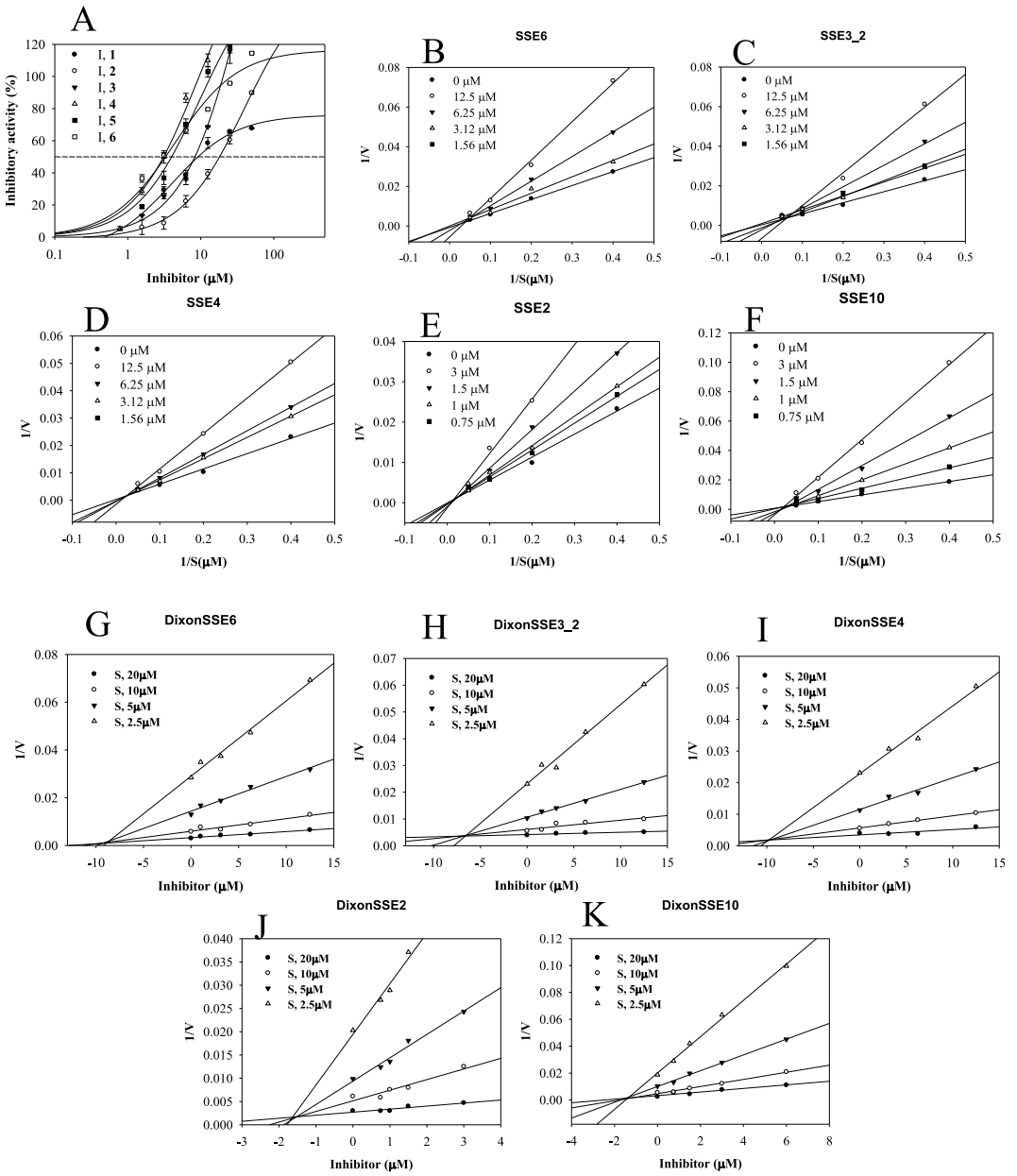

Fig. 3. Inhibitory activity (A), Lineweaver-burk plots (B–G) and Dixon plots (H–K) of compounds compounds **1**–**5** toward sEH.

and 2.88 Å, and Pro371 at 2.76 Å and 3.00 Å), three (Tyr343 at 2.71 Å, Ile363 at 3.01 Å, and Pro371 at 2.71 and 2.86 Å), two (Ast335 at 2.83 Å, and Leu408 at 2.87 Å and 3.11 Å), and six (Asp335 at 2.59 Å, Tyr383 at 2.81 Å, Gln384 at 2.93 Å, Ile363 at 2.98 Å, Trp473 at 2.85 Å, and Met469 at 2.57 Å) hydrogen bonds with amino acid residues, respectively (Fig. 4B–F).

3.4. Molecular dynamics prediction of the inhibitor–sEH binding sites

Molecular dynamics were performed to calculate the interaction of the potential inhibitors **4** and **5** with sEH in a flexible state. The two inhibitors–sEH simulated for 30 s were superimposed by deriving the results at 3 ns intervals, respectively (Fig. 5A and B). They were stable in the active site and exhibited a flexible movement with about -3.32×10^6 kJ/mol potential energy (Fig. 5C). The protein-based root-mean-square deviation (RMSD) and root-mean square deviation (RMSF) values of protein by ligands **4** and **5** were within 0.25 nm, respectively (Fig. 5D and E). Furthermore, Furthermore, compound **4** maintained 1–2 hydrogen bonds with amino acids and compound **5** maintained 4–6 hydrogen bonds, respectively (Fig. 5F and G). In particular, for 30 ns simulation time, the compound **4** maintained a ~3.5 Å distance with Tyr383, and compound **5** also maintained ~3.5 Å distance with four key amino acids

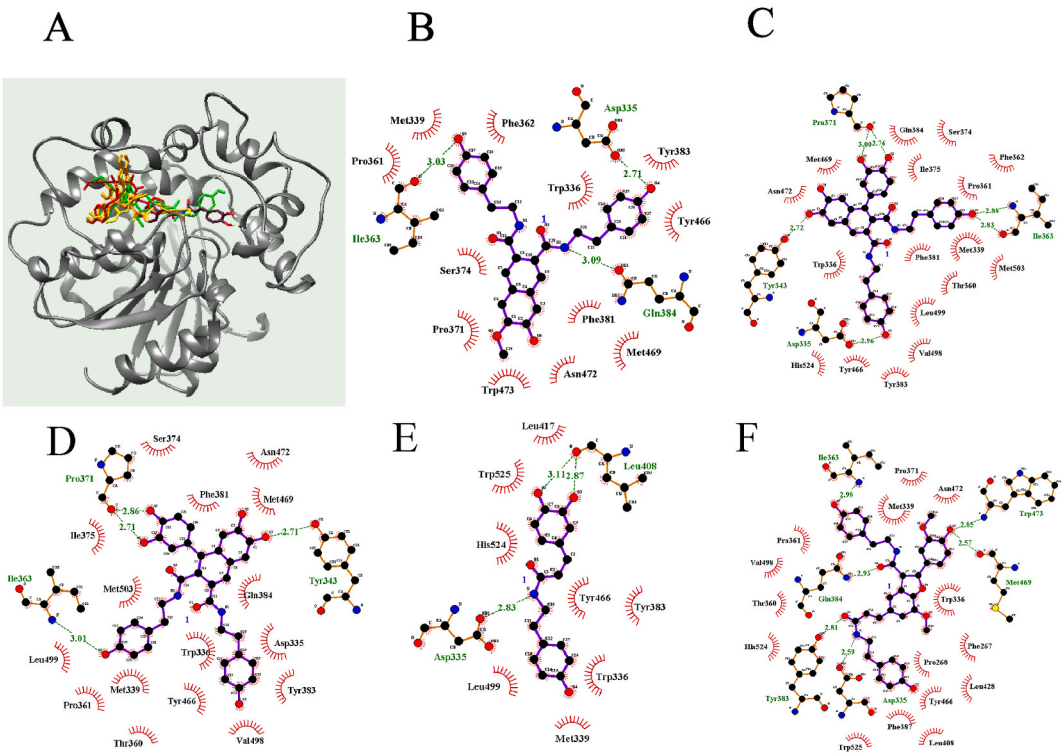

Fig. 4. The best pose (A) and the hydrogen bond interactions of the active site in EH with lignanamides **1**–**5** (B–F).

(Asp335, Tyr383, Tyr466, Asn472) (Fig. 5H–L).

4. Discussion

In the present study, we isolated lignanamides from hemp seed hulls for the development of a naturally derived sEH inhibitor. The first strong, stable sEH inhibitor was developed in 1999, following which the urea-based inhibitors AUDA, CPU (N-cyclohexyl-N′-(3-phenyl)propylurea), and TPPU (N-[1-(1-oxopropyl)-4-piperidinyl]-N′-[4-(trifluoromethoxy) phenyl]urea) have been considered as representative sEH inhibitors [18]. Amide analogues have also been developed as sEH inhibitors via organic synthesis [18] and from natural products [15,19], and lignanamides are structurally similar to some of these sEH inhibitors (e.g., TPNC, MTCMB, S-PPU, and *t*-TUCB) [18].

Hemp seed extracts were previously studied for their ability to suppress lipopolysaccharide (LPS)-induced interleukin (IL)-1β, IL-6, and tumor necrosis factor (TNF)-α expression in mice; the defatted ethanol extract was found to contain phenylpropionamides, *N-trans*-caffeoyltyramine, cannabisin A, and cannabisin B [20,21]. Moreover, in LPS-treated BV2 microglial cells, lignanamides (phenylpropionamides), coumaroyl-amino butanol glucopyranoside, 3,3′-demethyl-grossamide, and cannabisin G exerted anti-neuroinflammatory activities at concentrations of 15 μmol via TNF-α suppression [20,21]. *N-trans*-Coumaroyltyramine and *N-trans*-feruloyltyramine, derived from the leaves of *Capsicum chinense*, have also been reported to show competitive inhibition against sEH [10].

Following previous research, and employing bioactivity-guided fractionation, we observed high degrees of sEH inhibition by hemp seed hull ethanol extract (37.4 ± 1.2% at 50 μg/mL) and the ethyl acetate fraction (>100% at 50 μg/mL) thereof. The ethyl acetate fraction contained high concentrations of lignanamides, and one new (**1**) and four known (**2**–**5**) compounds were purified via column chromatography. All five compounds (**1**–**5**) had IC_{50} values of 3.2 ± 0.4–18.3 ± 1.0 μM with competitive mode against sEH activity via binding to the active site of the enzyme. Also, they had K_i value ranging of 1.5 ± 0.2–9.9 ± 0.8 μM. Compounds **1**–**3** and **5** had molecular weights exceeding 500 Da, and each bound across the active site and right pocket of sEH(ASN472). Meanwhile, compound **4** (molecular weight, ~300 Da) was an appropriate size for binding the active site. In particular, it was confirmed that potential inhibitors **4** and **5** in a fluid state maintain binding while stably interacting with sEH. In common, the two compounds maintained continuous hydrogen bonding between the ketone of the amide and Tyr383, and compound **5** with various functional groups formed additional hydrogen bonding with Asn472, Asp335, and Tyr466. Overall, it was confirmed that the ~300 Da lignanamide was a sufficient backbone for the development of sEH inhibitors through previously known sEH inhibitors [10] and compound **4**, and additionally, the possibility of ~500 Da compound **5** as a new lead compound was confirmed. These findings support the development of novel naturally derived sEH inhibitors.

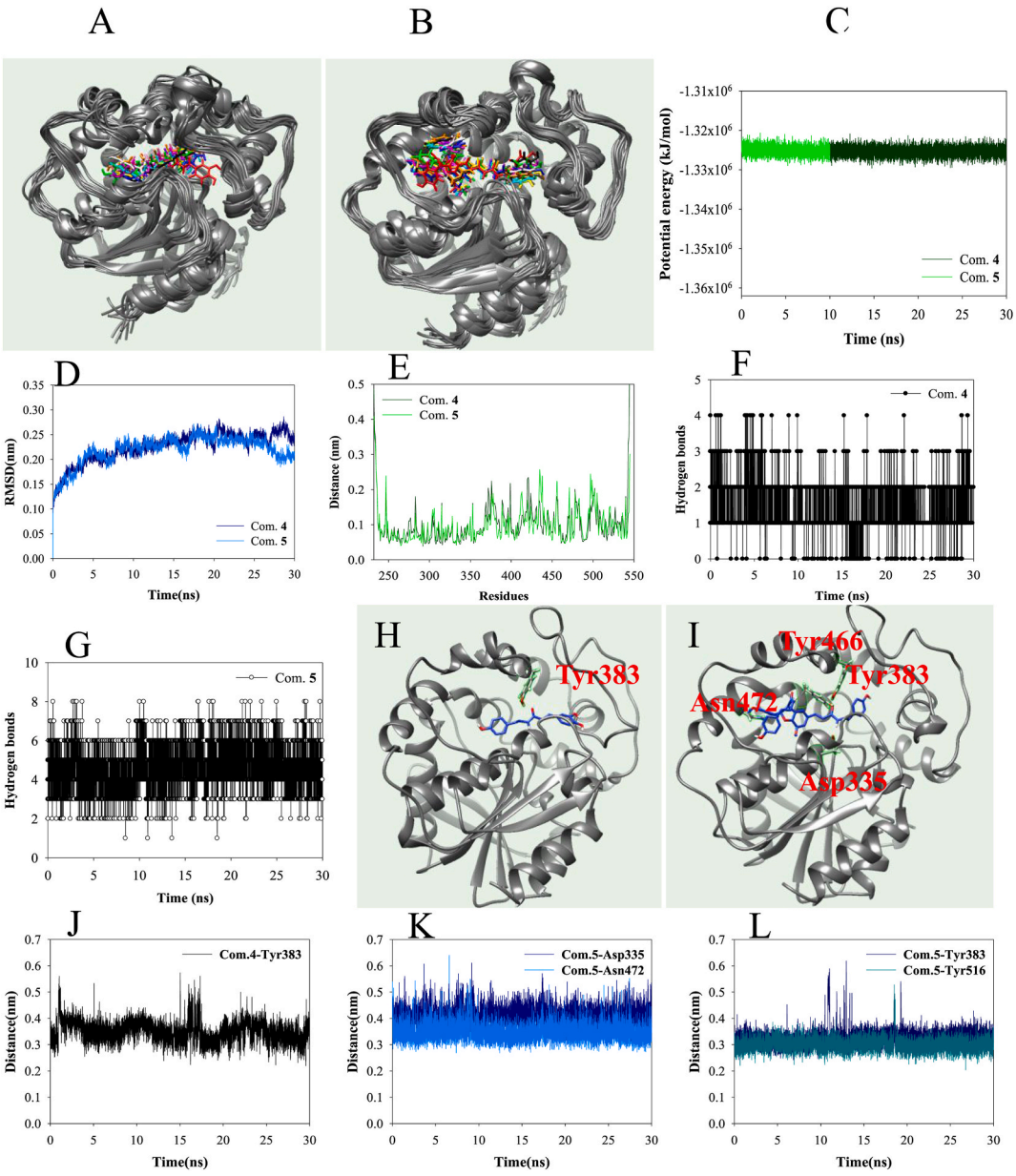

Fig. 5. The overlapped pose of inhibitors **4** (A) and **5** (B) with sEH for 30 ns(red: 0 ns, orange: 3 ns, yellow: 6 ns, green: 9 ns, cyan: 12 ns, blue: 15ns, conflower blue: 18 ns, purple: 21 ns, menganta: 24 ns, white: 27 ns, black: 30 ns). The potential energy (C), RMSD (D), RMSF (E), hydrogen bonds (F and G), of the simulation. The distance of key amino acids with inhibitors **4** (H and J) and **5** (I, K and L).

5. Conclusion

Among raw materials derived from hemp seeds, the hulls showed the greatest inhibitory activity against sEH. One new (**1**) and four known (**2**–**5**) lignanamides were isolated via silica gel and C-18 column chromatography from the ethyl acetate fraction of the hemp seed hull ethanol extract. Compounds **1**–**5** inhibited sEH activity (IC_{50}: 8.9 ± 08, 18.3 ± 1.0, 8.3 ± 1.1, 3.2 ± 0.4, and 3.3 ± 0.3 μM, respectively) via competitive binding (k_i: 9.0 ± 0.8, 6.9 ± 0.7, 9.9 ± 0.8, 1.8 ± 0.4, and 1.5 ± 0.2 μM, respectively). Computational chemistry revealed the amino acid residues most likely to participate in the hydrogen bonding of the inhibitors with sEH. The present study confirms the inhibitory activities of lignanamides against sEH, and reveals hemp seed hulls to be a natural source of raw materials. These findings are expected to support the development of novel sEH-targeting drugs for anti-inflammatory and cardiovascular diseases.

Author contribution statement

Jang Hoon Kim: Conceived and designed the experiments; Performed the experiments; Analyzed and interpreted the data; Contributed reagents, materials, analysis tools or data; Wrote the paper.

Yun-Chan Huh; Mok Hur; Woo Tae Park; Youn-Ho Moon; Tae IL Kim; Sung-Cheol Koo: Contributed reagents, materials, analysis tools or data;

Seon Mi Kim: Performed the experiments.

Data availability statement

No data was used for the research described in the article.

Declaration of competing interest

The authors declare that they have no known competing financial interests or personal relationships that could have appeared to influence the work reported in this paper.

Acknowledgement

This study was supported by the cooperative Research Program (RS-2022-RD010270 (PJ01701502)) of Rural Development Administration, Republic of Korea.

Appendix A. Supplementary data

Supplementary data to this article can be found online at https://doi.org/10.1016/j.heliyon.2023.e19772.

References

[1] C. Benkirane, A.B. Moumen, M.-L. Fauconnier, K. Belhaj, M. Abid, H.S. Caid, A. Elamrani, F. Mansouri, Bioactive compounds from hemp (*Cannabis sativa* L.) seeds: optimization of phenolic antioxidant extraction using simplex lattice mixture design and HPLC-DAD/ESI-MS2 analysis, RSC Adv. 12 (2022), 25764.
[2] M.T. Welling, M.A. Deseo, A. Bacic, M.S. Doblin, Biosynthetic origins of unusual cannabimimetic phytocannabinoids in Cannabis sativa L: a review, Phytochemistry 201 (2022), 113282.
[3] R. Yang, E.C. Berthold, C.R. McCurdy, S.d.S. Benevenute, Z.T. Brym, J.H. Freeman, Development of cannabinoids in flowers of industrial hemp (*Cannabis sativa* L.): a pilot study, J. Agric. Food Chem. 68 (22) (2020) 6058–6064.
[4] V. Menga, C. Garofalo, S. Suriano, R. Beleggia, S.A. Colecchia, D. Perrone, M. Montanari, N. Pecchioni, C. Fares, Phenolic acid composition and antioxidant activity of whole and defatted seeds of Italian hemp cultivars: a two-year case study, Agriculture 12 (2022) 759.
[5] W. Huang, Z. Zeng, Y. Lang, X. Xiang, G. Qi, G. Lu, X. Yang, Cannabis seed oil alleviates experimental atherosclerosis by ameliorating vascular inflammation in apolipoprotein-E-deficient mice, J. Agric. Food Chem. 69 (2021) 9102–9110.
[6] J.R. Martinez, G. Šelo, M.A. Fernández-Arche, B. Bermudez, M.D. García-Giménez, Dual role of phenyl amides from hempseed on BACE 1, PPARγ, and PGC-1α in N2a-APP cells, J. Nat. Prod. 84 (2021) 2447–2453.
[7] X. Yan, J. Tang, C.d.S. Passos, A. Nurisso, C.A.M.J. Simoes-Pires, H. Lou, P. Fan, Characterization of lignanamides from hemp (*Cannabis sativa* L.) seed and their antioxidant and acetylcholinesterase inhibitory activities, J. Agric. Food Chem. 63 (2015) 10611–10619.
[8] K.M. Wagner, C.B. McReynolds, S.W.K. Chmidt, B.D. Hammock, Soluble epoxide hydrolase as a therapeutic target for pain, inflammatory and neurodegenerative diseases, Pharmacol. Ther. 180 (2017) 62–76.
[9] C.-P. Sun, X.-Y. Zhang, C. Morisseau, S.H. Hwang, Z.-J. Zhang, B.D. Hammock, X.-C. Ma, Discovery of soluble epoxide hydrolase inhibitors from chemical synthesis and natural products, J. Med. Chem. 64 (2021) 184–215.
[10] J.D. Imig, B.D. Hammock, Soluble epoxide hydrolase as a therapeutic target for cardiovascular diseases, Nature 8 (2009) 794–805.
[11] Y. Wang, K.M. Wanger, C. Morisseau, B.D. Hammock, Inhibition of the soluble epoxide hydrolase as an analgesic strategy: a review of preclinical evidence, J. Pain Res. 14 (2021) 61–72.
[12] N. Tripathi, S. Paliwal, S. Sharma, K. Verma, R. Gururani, A. Tiwari, A. Verma, M. Chauhan, A. Singh, D. Kumar, A. Pant, Discovery of novel soluble epoxide hydrolase inhibitors as potent vasodilators, Sci. Rep. 8 (2018), 14604.
[13] M. Manickam, S. Meenakshisundaram, T. Pillaiyar, Activating endogenous resolution pathways by soluble epoxide hydrolase inhibitors for the management of COVID-19, Arch. Pharm. 355 (2022), e2100367.
[14] D. Panigraphy, M.M. Gilligan, S. Huang, A. Gratung, I. Cortés-Puch, P.J. Sime, R.P. Phipps, C.N. Serhan, B.D. Hammock, Inflammation resolution: a dual-pronged approach to averting cytokine storms in COVID-19? Cancer Metastasis Rev. 39 (2020) 337–340.
[15] J.H. Kim, Y.D. Jo, H.-Y. Kim, B.-R. Kim, B. Nam, *In vitro* and *in silico* insights into she inhibitor siwth amide-scaffold from the leaves of *Capsicum chinense* Jacq, Comput. Struct. Biotechnol. J. 16 (2018) 404–4011.
[16] I. Sakakibara, T. Katsuhara, Y. Ikeya, K. Hayashi, H. Mitsuhashi, A. Cannabisin, An arylnaphthalene lignanamide from fruits of *cannabis staiva*, Phytochemistry 30 (9) (1991) 3013–3016.
[17] T. Chen, J. He, J. Zhang, X. Li, H. Zhang, J. Hao, L. Li, The isolation and identification of two compounds with predominant radical scavenging activity in hempseed (seed of *Cannabis sativa* L.), Food Chem. 134 (2012) 1030–1037.
[18] C.-P. Sun, X.-Y. Zhang, Discovery of soluble epoxide hydrolase inhibitors from chemical synthesis and natural products, J. Med. Chem. 64 (2021) 184–215.
[19] Z.B. Liu, C.P. Sun, J.X. Xu, C. Morisseau, B.D. Hammock, F. Qiu, Phytochemical constituents from *Scutellaria baicalensis* in soluble epoxide hydrolase inhibition: kinetics and interaction mechanism merged with simulations, Int. J. Biol. Macromol. 133 (2019) 1187–1193.
[20] Y. Zhou, S. Wang, J. Ji, H. Lou, P. Fan, Hemp (*Cannabis sativia* L.) seed phenylpropionamides composition and effects on memory dysfunction and biomarkers of neuroinflammation induced by lipopolysaccharide in mice, ACS Omega 3 (2018) 15988–15995.
[21] Y. Zhou, S. Wang, H. Lou, P. Fan, Chemical constituents of hemp (*Cannabis sativa* L.) seed with potential anti-neuroinflammatory activity, Phytochem. Lett. 23 (2018) 57–61.